

PCCCP

Physical Chemistry Chemical Physics

Accepted Manuscript

This article can be cited before page numbers have been issued, to do this please use: S. P. Pinho, A. Alhadid, M. Minceva and J. A.P. Coutinho, *Phys. Chem. Chem. Phys.*, 2026, DOI: 10.1039/D6CP00187D.



This is an Accepted Manuscript, which has been through the Royal Society of Chemistry peer review process and has been accepted for publication.

Accepted Manuscripts are published online shortly after acceptance, before technical editing, formatting and proof reading. Using this free service, authors can make their results available to the community, in citable form, before we publish the edited article. We will replace this Accepted Manuscript with the edited and formatted Advance Article as soon as it is available.

You can find more information about Accepted Manuscripts in the [Information for Authors](#).

Please note that technical editing may introduce minor changes to the text and/or graphics, which may alter content. The journal's standard [Terms & Conditions](#) and the [Ethical guidelines](#) still apply. In no event shall the Royal Society of Chemistry be held responsible for any errors or omissions in this Accepted Manuscript or any consequences arising from the use of any information it contains.

The Melting Properties of Choline Chloride in the Representation of Deep Eutectic Systems Phase Diagrams

View Article Online
DOI: 10.1039/D6CP00187D

Ahmad Alhadid¹, Mirjana Minceva², João A. P. Coutinho³, Simão P. Pinho⁴

¹ College of Engineering and Technology, American University of the Middle East, Kuwait

² Biothermodynamics, TUM School of Life Sciences, Technical University of Munich, Freising, Germany

³ CICECO – Aveiro Institute of Materials, Department of Chemistry, University of Aveiro, 3810-193 Aveiro, Portugal

⁴ CIMO-Mountain Research Center, LA SusTEC, Bragança Polytechnic University, Campus of Santa Apolónia, Bragança, Portugal

*Corresponding author: Simão P. Pinho

Telephone: +351 273 303 086

Fax: +351 273 313 051

E-mail: spinho@ipb.pt



Abstract

View Article Online

DOI: 10.1039/D6CP00187D

Choline chloride (ChCl) is the cornerstone of deep eutectic solvents (*DES*), yet its melting properties remain an important source of uncertainty in the thermodynamic description of eutectic systems. Since ChCl decomposes before melting, reported values of its melting temperature (597 to 687 K) and enthalpy (4.3 and 13.8 kJ mol⁻¹) vary widely, while for the heat capacity change between solid and liquid states, only an estimate exists at 298.15 K. All these factors propagate inconsistencies into solid-liquid equilibrium (SLE) modelling, activity coefficient estimation, and data-driven approaches such as machine learning. In this work, we critically assess the melting properties of ChCl reported in the literature and evaluate their impact on the representation of phase diagrams of eutectic systems. By analysing the description of representative binary systems (ChCl + ionic compound, ChCl + water, and ChCl + urea), we demonstrate that neglecting the heat capacity change upon melting can lead to a substantial underestimation of the melting enthalpy. Thermodynamic modelling using NRTL-based approaches further reveals a strong interdependence between melting properties, liquid-phase nonideality, and the interpretation of experimental SLE data. Our results indicate that melting enthalpy values between 8-10 kJ mol⁻¹, combined with a non-negligible heat capacity change upon melting in the range 20-40 J mol⁻¹K⁻¹, provide the most consistent description across systems. This study clarifies the role of ChCl melting properties in the thermodynamic description of eutectic systems, providing a robust framework for enhancing the reliability of phase diagram interpretation, model development, and data-driven predictions in *DES* research.

Keywords: deep eutectic solvents, phase diagram, eutectic point, electrolyte systems, heat capacity change, melting enthalpy.



Introduction

View Article Online

DOI: 10.1039/D6CP00187D

Choline chloride (ChCl) is undoubtedly the most used substance in forming deep eutectic solvents (*DES*). The term *DES* emerged around 2003 when Abbott and co-authors proposed using ChCl-based eutectic mixtures as novel solvents.¹ In their pioneering work, they introduced the concept of employing eutectic mixtures characterised by a significant depression of the melting temperature as novel designer solvents, with ChCl + urea system serving as an example. Their work opened the door to the exploration of other systems and quickly expanded the field for applications in many areas of technology, including metal extraction, distillation or liquid-liquid extraction, biocatalysis, biomass processing, and the development of vehicles for the solubilization, transport, and bioavailability of active ingredients in the pharmaceutical industry, among others.^{2,3}

In 2018, a proposal was made to establish a clear basis for the terminology related to *DES*, aiming to prevent ambiguities and ensure the use of scientifically accurate terms.⁴ In that paper, the importance of measuring the solid-liquid equilibria (SLE) phase diagram of these mixtures was highlighted. It was also shown how significant it is to know the properties of *DES* constituents, such as melting temperature, melting enthalpy, and heat capacities at both liquid and solid phases, which are often not directly accessible through experiments using calorimetric techniques. This is the case with ChCl, which decomposes before melting. While a few “experimental” values of the melting temperature are available, varying from 575.15 to 588.75 K (sometimes reporting issues related to decomposition),^{1,5,6} the first value for the melting enthalpy, estimated by an indirect method, was published in 2017.⁷

Accurate knowledge of the melting properties of *DES* constituents is essential to correctly evaluate the system thermodynamic behaviour and quantify deviations from ideality. Activity coefficients are key parameters in the thermodynamic modelling of *DES*, and inaccurate data can lead to both poor and seemingly good predictions, potentially resulting in misleading conclusions about a model’s ability to describe SLE in *DES*. Furthermore, as machine learning (ML) becomes increasingly integrated into this field,^{8,9} the importance of reliable melting properties and high-quality SLE data continues to grow. Melting properties are also critical for assessing the quality and consistency of published experimental datasets.¹⁰

As many *DES* are composed of ChCl, the work by Fernandez et al.⁷ contributed to developing new perspectives in this field. Starting from the concepts of colligative properties, Pyykko¹¹ proposed an empirical approach to estimate the eutectic point, while Kollau et al.¹² developed a strategy to assess the composition range of mixtures that remain in the liquid state at room



temperature. On the other hand, Alhadid et al.¹³ used a parametric study confirming the extreme importance of the melting properties of the *DES* constituents in understanding and designing new *DES* systems. The authors showed that due to the interrelation between the melting properties and the activity coefficients of the *DES* components, the SLE phase diagrams of a *DES* can be effectively described by adjusting different melting enthalpy values. Lower melting enthalpies resulted in behavior that closely approximates an ideal liquid phase, whereas higher values require the inclusion of activity coefficients to compensate for the high melting enthalpies and appropriately describe the SLE .

Applying the COSMO-RS model, Song et al.¹⁴ showed that the accuracy of the model to represent SLE in eutectic systems depends heavily on the salt conformer choice, yielding reasonable eutectic temperature predictions but less accurate eutectic composition estimates, while Peng et al.¹⁵ reported the inability to accurately predict SLE in salt-based eutectic systems, whether the salt was modeled as an ion pair or fully dissociated. This inaccuracy stems from both limitations in the model and unreliable melting data for thermally unstable salts.

Different methods for modelling phase equilibria and properties of deep eutectic solvents *DES*, including excess Gibbs energy (G^E) models, equations of state (EoS), and molecular dynamics (MD) simulations, have been applied.¹⁶ Some G^E models and EoS approaches often treat *DES* as pseudo-components to simplify parameterization and calculations, limiting their applicability, while the use of group-contribution models such as UNIFAC¹⁷⁻¹⁹ makes the approach more general, increasing the parameter transferability to other systems. More recently, a line of work combining thermodynamics and ML has been receiving enormous attention. Specifically for predicting SLE phase diagrams and eutectic coordinates in systems containing salts such as ChCl, the melting temperature and enthalpy of the pure components are again important molecular descriptors.²⁰ However, the experimental difficulties associated with their determination, particularly for alkylammonium-based halides, make it very difficult to compute the melting point of *DES* accurately, as shown by Ayres et al.,²¹ where all the melting point prediction outliers are from mixtures containing compounds such as ChCl. As the ML models for eutectic coordinates depend heavily on the melting properties of *DES* constituents and activity coefficients,²² further efforts are necessary for the accurate systematization of the SLE experimental data, as reported in the review from López-Flores et al.²³ These experimental difficulties for measuring the SLE phase diagrams altogether with the melting properties uncertainty of the pure ChCl leads to very different conclusions in terms of the eutectic coordinates, as recently discussed for ethylene glycol + ChCl mixture.²⁴ For ChCl in particular, the published melting temperatures vary from 575.15 K to 687 K,^{1, 24} while the melting enthalpy



is in the range 4.3-13.8 kJ mol⁻¹.^{7, 24} To the best of our knowledge, only an estimate for the heat capacity upon melting is available at 298.15 K, which is 39.3 J mol⁻¹K⁻¹.²⁵

View Article Online

DOI: 10.1039/D6CP00187D

In this context, this paper critically reviews and discusses the various melting properties of ChCl reported in the open literature. It presents a detailed evaluation of data, comparing and testing different published values and their impact on the representation of binary phase diagrams of ChCl with ionic compounds, water, or urea, firstly considering the ideality of the liquid phase. In a complementary perspective, this systematic investigation is further deepened using NRTL-based approaches to model different thermodynamic properties and SLE of the systems ChCl + water and ChCl + urea, analyzing the influence of ChCl melting properties on the phase diagram representations and liquid phase nonideality quantification, performing a sensitivity analysis.

ChCl Melting Properties

ChCl exhibits several notable structural characteristics. It is a quaternary ammonium salt composed of a bulky choline cation and a small chloride anion, resulting in significant charge asymmetry. The chloride ion has a high charge density, whereas the choline cation features a positively charged nitrogen center and a hydroxyl group capable of hydrogen bonding. This combination imparts a dual character: high polarity and the capacity for both strong ionic and hydrogen-bonding interactions, occurring intra- and intermolecularly. These interactions explain ChCl's well-defined solid-solid phase transition and relatively high melting temperature compared to many organic compounds, although it seems to melt at a lower temperature than typical inorganic salts. Additionally, this structural makeup accounts for its pronounced hygroscopic nature. While the solid-solid transition between α and β phases is well-defined, reversible, and associated with high enthalpy and entropy changes,²⁵ the melting is not well-defined. Besides the plastic crystalline character of the β phase,²⁶ the tendency to undergo irreversible changes, decomposition at high temperatures, and its strong hygroscopic nature complicates both the experimental handling and the interpretation of phase behavior data.

Short Historical Perspective

For eutectic systems with complete immiscibility in the solid phase, a solid-solid transition, and a constant heat capacity change upon melting, the solid-liquid equilibrium can be described by:²⁷



$$\ln x_i \gamma_i = \frac{\Delta H_{m,i}}{RT} \left(\frac{T}{T_{m,i}} - 1 \right) + \frac{\Delta H_{tr,i}}{RT} \left(\frac{T}{T_{tr,i}} - 1 \right) - \frac{\Delta C_{p,m,i}}{R} \left(1 - \frac{T_{m,i}}{T} + \ln \frac{T_{m,i}}{T} \right) - \frac{\Delta C_{p,tr,i}}{R} \left(1 - \frac{T_{tr,i}}{T} + \ln \frac{T_{tr,i}}{T} \right) \quad (1)$$

where x_i is the mole fraction solubility of compound i and γ_i its activity coefficient in the liquid phase, $\Delta H_{m,i}$ and $T_{m,i}$ are the molar melting enthalpy and temperature, $\Delta H_{tr,i}$ and $T_{tr,i}$ the solid-solid molar transition enthalpy and temperature, R is the ideal gas constant, T is the absolute temperature, and $\Delta C_{p,m,i}$ is the difference between the molar heat capacity of the compound i in liquid and solid phases, while $\Delta C_{p,tr,i}$ is its equivalent for the solid-solid transition.

If considering only data above the solid-solid transition temperature, neglecting the term related to the heat capacity change upon melting and assuming the liquid phase as an ideal mixture, Equation (1) becomes:

$$\ln x_i = \frac{\Delta H_{m,i}}{RT_{m,i}} + \frac{\Delta H_{m,i}}{RT} \quad (2)$$

Equation (2) served as the basis for the first estimation of the melting enthalpy of ChCl by Fernandez et al.,⁷ through the fitting of experimental SLE data. A large set of ionic systems was initially studied, from which ten were identified as forming ideal liquid solutions. Thermodynamic consistency tests recently proposed by NIST²⁸ and DTU²⁹ were applied to validate the experimental data. The systems that were considered ideal were selected based on the ChCl mole fraction ratios, at the same temperature, in two different binary systems, which are equivalent to activity coefficient ratios. These ratios ranged from 0.93 to 1.07, guaranteeing at least similar deviations from the ideal solution, further confirmed by calculating the activity coefficients by COSMO-RS.

Based on the assumptions of Equation (2) and using the SLE data of the ten selected systems, always above solid-solid transition temperature (351 ± 3 K),³⁰ the estimated melting temperature and enthalpy were 597 ± 7 K and 4.3 ± 0.6 kJ mol⁻¹, respectively. When applying a similar linear fit to the SLE data of each of the ten systems individually, the corresponding values fell within the range 589-632 K for the melting temperature and 3.7-5.5 kJ mol⁻¹ for the melting enthalpy.

Considering the value of solid-solid transition enthalpy (16.5 ± 0.2 kJ mol⁻¹)³⁰ at 351 K, the estimated melting enthalpy of 4.3 ± 0.6 kJ mol⁻¹ is remarkably low. Consequently, a



comprehensive study to measure the solubility of ten alkylammonium halide salts (chlorides and bromides) in water was started.³¹ Using density and water activity data of these binary mixtures, parameters for a PC-SAFT-based model were initially estimated. Using the PC-SAFT model to calculate the salt activity coefficients and combining them with experimental solubility data, the melting enthalpies of the salts were estimated, assuming a melting temperature of 597 K and neglecting heat capacity contributions. For ChCl, the estimated melting enthalpy for a melting temperature of 597 K was 7.8 kJ mol⁻¹.³¹

In 2023, using ultra-fast scanning calorimetry in combination with micro X-ray diffraction and high-speed optical microscopy, van den Bruinhorst et al.²⁴ measured the melting temperature and enthalpy of ChCl, reporting values of 687 ± 9 K and 13.8 ± 3.0 kJ mol⁻¹, respectively. These data differ significantly from previously estimated values, highlighting the need for further studies. An initial contribution in this direction was made by Correa et al.,³² who simulated the phase transitions of ChCl using different atomistic force fields through molecular dynamics. Although the limited availability of experimental data for the liquid phase of ChCl and the high sensitivity to the choice of force field constrain the accuracy of these computational approaches, their study suggests a melting temperature of 627 K and a melting enthalpy of 7.8 kJ mol⁻¹. Table 1 summarizes the published values of the melting properties of ChCl.

Table 1. Compilation of the melting temperature and enthalpy of choline chloride, method and sources.

T_m / K	$\Delta H_m / \text{kJ mol}^{-1}$	Method	Reference
597 ± 7	4.3 ± 0.6	ChCl solubility on binary ideal systems	Fernandez et al. ⁷
597	7.8	ChCl solubility in water + PC-SAFT	Vilas-Boas et al. ³¹
687 ± 9	13.8 ± 3.0	Fast-DSC on pure ChCl	Bruinhorst et al. ²⁴
627	7.8	Molecular Dynamics on pure ChCl	Correa et al. ³²

Heat capacity Impact

Because changes in heat capacity upon melting are often unknown, they are typically neglected in calculations. While this omission usually has only a minor effect on solubility estimates, it can become significant when the enthalpy of melting is small, and there is a large temperature difference between the mixture's melting point and that of the pure compound. That is the case with most of the SLE phase diagrams of binary mixtures containing ChCl. For this reason, Equation (2) should more correctly keep the heat capacity term and be written as:



$$\ln x_i = \frac{\Delta H_{m,i}}{RT} \left(\frac{T}{T_{m,i}} - 1 \right) - \frac{\Delta C_{p,m,i}}{R} \left(1 - \frac{T_{m,i}}{T} + \ln \frac{T_{m,i}}{T} \right) \quad (3)$$

View Article Online
DOI: 10.1039/D6CP00187D

Figure 1 illustrates the average weight percentage, defined as the ratio of the heat capacity term value to the total value of the right-hand side of Equation (3), which encompasses both enthalpy and heat capacity terms contributions. This weight is calculated as an average in the temperature interval from the solid-solid transition temperature (351 K) and the fixed melting temperature of ChCl (600 or 700 K). This temperature range was selected to match the temperature interval of the experimental data of the binary ionic systems initially used to estimate the ChCl melting properties via Equation (2). Due to the uncertainty of the melting properties of ChCl (see Table 1), the calculations were carried out at two melting temperatures (600 and 700 K) and three different melting enthalpies (4, 8 and 14 kJ mol⁻¹) within the range of published melting properties, varying the heat capacity change from 0 to 50 J mol⁻¹K⁻¹. As expected, the contribution of the heat capacity term increases with the decrease in melting enthalpy and the increase in melting temperature. In the context of this work, it is important to highlight that at the lowest melting enthalpy (4 kJ mol⁻¹), the heat capacity term shows an average weight percentage higher than 25% for $\Delta C_{p,m} = 20$ J mol⁻¹K⁻¹ and increases to 40% for $\Delta C_{p,m} = 40$ J mol⁻¹K⁻¹, which is a very likely $\Delta C_{p,m}$ value. At this same $\Delta C_{p,m}$ value, even at a melting enthalpy of 14 kJ mol⁻¹, that average weight percentage is as high as 20%.



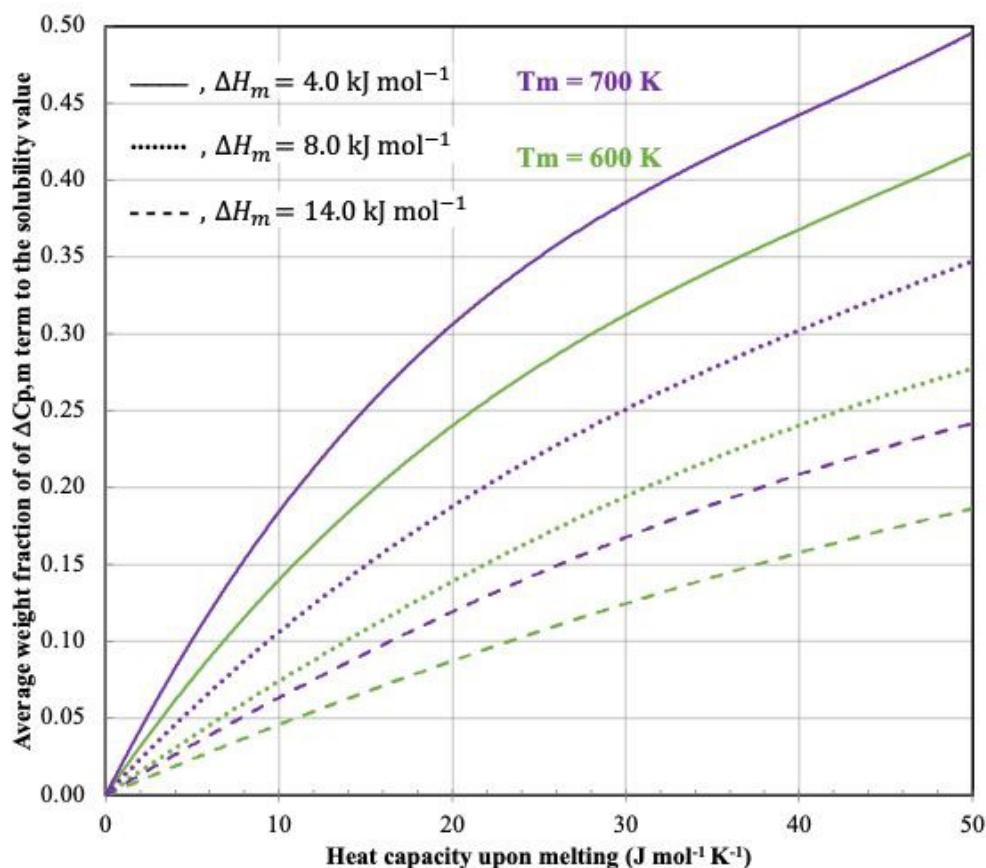


Figure 1. Average weight percentage of the heat capacity term in the SLE Equation (1) for choline chloride, depending on the heat capacity change upon melting, at different melting temperatures.

For the lowest value of the melting enthalpy (4 kJ mol^{-1}) in Figure 1, neglecting the heat capacity term can be a critical simplification. Given that the first reported⁷ ChCl melting enthalpy is 4.3 kJ mol^{-1} , which was estimated by neglecting the heat capacity term, it is essential to explore how neglecting that term may have influenced the estimated value for the ChCl enthalpy of melting. Considering the ideality of the liquid phase again and using Equation (3), hypothetical solubility lines for ChCl were calculated between the solid-solid transition temperature and a fixed melting temperature (600 or 700 K), across a range of heat capacities ($0\text{-}50 \text{ J mol}^{-1}\text{K}^{-1}$) and melting enthalpies ($0\text{-}40 \text{ kJ mol}^{-1}$). These hypothetical solubility values were obtained by linearizing Equation 2, and new melting enthalpy and temperature values were estimated, neglecting, for comparison purposes, the heat capacity term.

Figure 2 illustrates the decrease in the calculated melting enthalpy at two different melting temperatures, compared to a fixed melting enthalpy value used in Equation (2). This is the most significant result of this analysis, as the estimated enthalpy of melting is consistently higher than



the fixed value, and this increment grows linearly with the heat capacity change (Figure 2). To better understand the relevance of Figure 2, consider the following example for clarification. When $\Delta C_{p,m} = 30 \text{ J mol}^{-1}\text{K}^{-1}$ and $T_m = 600 \text{ K}$, the enthalpy of melting neglecting the $\Delta C_{p,m}$ term is underestimated by approximately 4 kJ mol^{-1} . Consequently, with an estimated temperature of 597 K ⁷ and considering $\Delta C_{p,m} = 30 \text{ J mol}^{-1}\text{K}^{-1}$, the real enthalpy would be 8.3 kJ mol^{-1} (4 kJ mol^{-1} above the first melting enthalpy value estimated by Fernandez et al.⁷). A similar underestimation of 4 kJ mol^{-1} is observed when $\Delta C_{p,m} = 20 \text{ J mol}^{-1}\text{K}^{-1}$ but $T_m = 700 \text{ K}$. The magnitude of this underestimation does not depend on the fixed value of the melting enthalpy, but only on the assumed value of the heat capacity change. With respect to the melting temperatures, the reestimated values are always slightly higher than the original values, more for lower melting enthalpies and higher $\Delta C_{p,m}$ values.

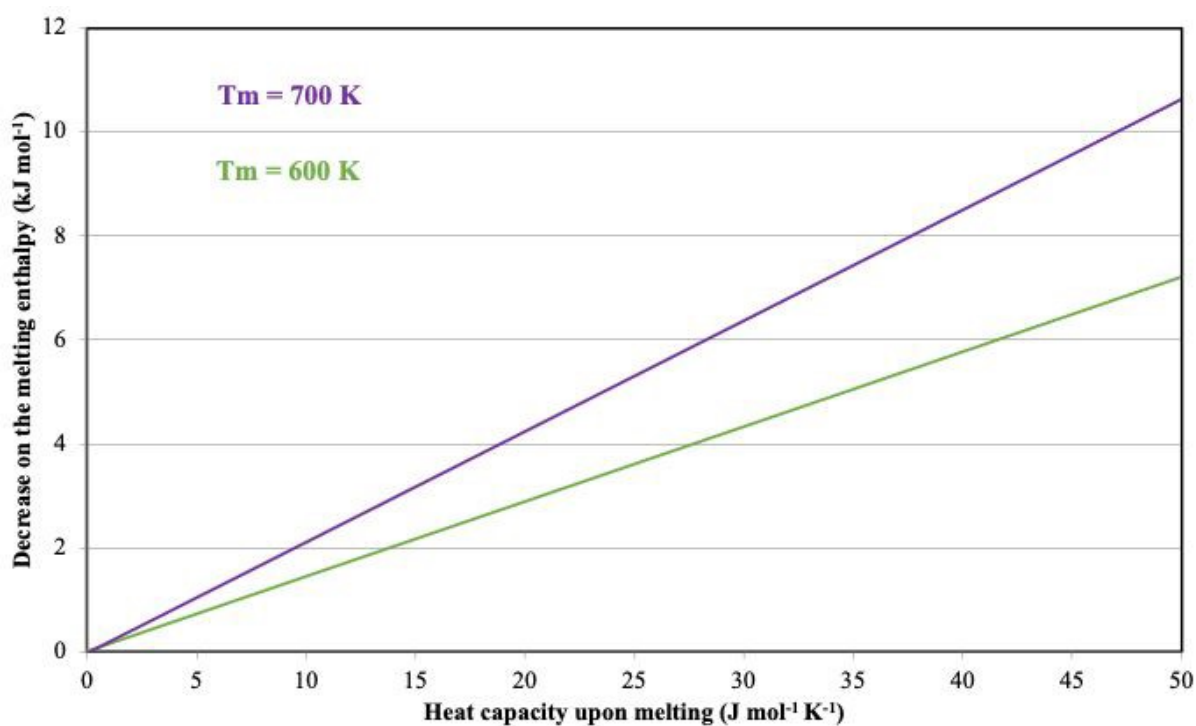


Figure 2. Melting enthalpy increment to be added to the melting enthalpy estimated from Equation (2), neglecting the heat capacity term.

Melting Properties in the Description of Ideal SLE Phase Diagrams

Ionic Binary Systems

Initially, the different sets of melting properties compiled in Table 1 were used in Equation (3) to calculate the ideal ChCl solubility line and compare it with the experimental data measured for binary salt mixtures containing ChCl.⁷ Figure 3(a) presents such a comparison, when



neglecting the $\Delta C_{p,m}$ term (Equation 2). Unsurprisingly, the best agreement was obtained using the values proposed by Fernandez et al.⁷ In contrast, when employing melting properties measured by Fast-DSC,²⁴ the deviations from the experimental data become notably significant.

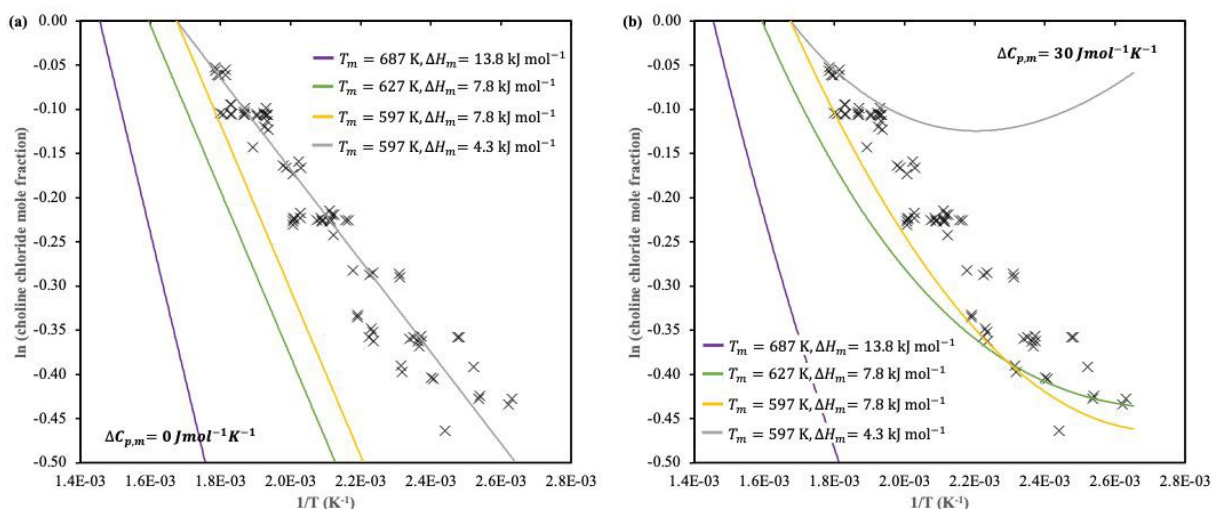


Figure 3. Representation of $\ln x_{\text{ChCl}}$ as a function of $1/T$: (a) $\Delta C_{p,m} = 0 \text{ J mol}^{-1} \text{ K}^{-1}$, (b) $\Delta C_{p,m} = 30 \text{ J mol}^{-1} \text{ K}^{-1}$, using the different melting properties compiled in Table 1: — Fernandez et al.⁷; — Vilas-Boas et al.³¹; — Bruinhorst et al.²⁴ and — Correa et al.³² The data points are from binary systems constituted by [Ch]Cl and [Ch][Ac], [Ch][Prop], [Ch][Buta], [N4444]Cl, [P4444]Cl, [BzCh]Cl, [C4mpyr]Cl, [Ch][NTf₂], [C₂mim]Cl or [C₂OHmim]Cl.⁷

In Figure 3(b), the predictions are carried out using Equation (3), with the value of $\Delta C_{p,m}$ fixed at $30 \text{ J mol}^{-1} \text{ K}^{-1}$. It is evident that the melting temperature and enthalpy reported by Fernandez et al.,⁷ when combined with this $\Delta C_{p,m}$ value, yield a representation of the liquidus line that lacks physical meaning. The calculated solubility line would also suggest strong positive deviations from ideality in these systems, which is not expected. On the other hand, the melting properties reported by van den Bruinhorst et al.²⁴ would indicate a significant negative deviation from ideality, even at ChCl mole fractions approaching one. This behavior is also not physically plausible since activity coefficients should tend toward unity under these conditions. Overall, the intermediate melting properties reported by Vilas-Boas et al.³¹ and Correa et al.³² provide a more consistent description of the experimental data when $\Delta C_{p,m}$ of $30 \text{ J mol}^{-1} \text{ K}^{-1}$ is considered.

ChCl + Neutral Molecule Systems

To evaluate the melting properties of ChCl on the description of other systems, the SLE phase diagrams of the binary ChCl + water and ChCl + urea systems were selected, given the amount and quality of data provided by various authors. Taking into account the range for the melting temperature and enthalpy reported in Table 1, and by selecting $\Delta C_{p,m}$ values ranging from 0 to $40 \text{ J mol}^{-1} \text{ K}^{-1}$, the phase diagrams were calculated by Equation (1), under the assumption of ideal behavior in the liquid phase and taking into account the ChCl solid-solid transition. All



other properties needed for these calculations are well-established, such as the melting properties of water ($\Delta H_{\square} = 6.01 \text{ kJ mol}^{-1}$ and $T_{\square} = 273.2 \text{ K}$), urea ($\Delta H_{\square} = 14.6 \text{ kJ mol}^{-1}$, $T_{\square} = 407.2 \text{ K}$), and for the ChCl the solid-solid (ss) transition properties ($T_{ss} = 352.2 \text{ K}$, $\Delta H_{ss} = 16.3 \text{ kJ mol}^{-1}$ and $\Delta C_{p,ss} = 16 \text{ J mol}^{-1}\text{K}^{-1}$).²⁵

ChCl + water system

Despite that in the *DES* study, the COSMO-RS model showed limited accuracy in capturing the temperature effect on the activity coefficients, at 298.15 K, it provided a reliable approximation for the activity coefficients of water in the presence of ChCl, derived from water activity measurements, indicating, at the same time, that the activity coefficient of ChCl is close to unity for ChCl mole fractions above 0.5.²⁵ Encouraged by this near-ideal behavior of ChCl, predictions of SLE phase diagrams by varying ChCl melting properties were compared against the experimental data to assess their reliability.

First, the melting temperature and enthalpy from Table 1 are used to explore the impact of introducing the $\Delta C_{p,m}$ term. When the change in heat capacity upon melting is neglected (Figure 4a), none of the available data sets adequately represent the solubility line of ChCl. The data reported by Fernandez et al.⁷ yield an unexpected positive deviation at higher temperatures, and a negative deviation below the solid–solid transition temperature. With $\Delta C_{p,m} = 20 \text{ J mol}^{-1}\text{K}^{-1}$ (Figure 4b) the magnitude of the negative deviation from ideality is significantly reduced. For the intermediate enthalpy value,^{31, 32} a small positive deviation from ideality at temperatures above the solid-solid transition temperature, and a physically implausible liquidus line are obtained when using the melting properties data from Fernandez et al.⁷ This inconsistency becomes more pronounced with $\Delta C_{p,m} = 40 \text{ J mol}^{-1}\text{K}^{-1}$ (Figure 4c), where only the data from van den Bruinhorst et al.²⁴ yield a plausible representation of the solubility line. In all cases, increasing $\Delta C_{p,m}$ shifts the eutectic composition toward higher ChCl concentrations, and the evident discrepancy of the eutectic temperature to the experimental value becomes lower, but grows with increasing values of the melting properties.



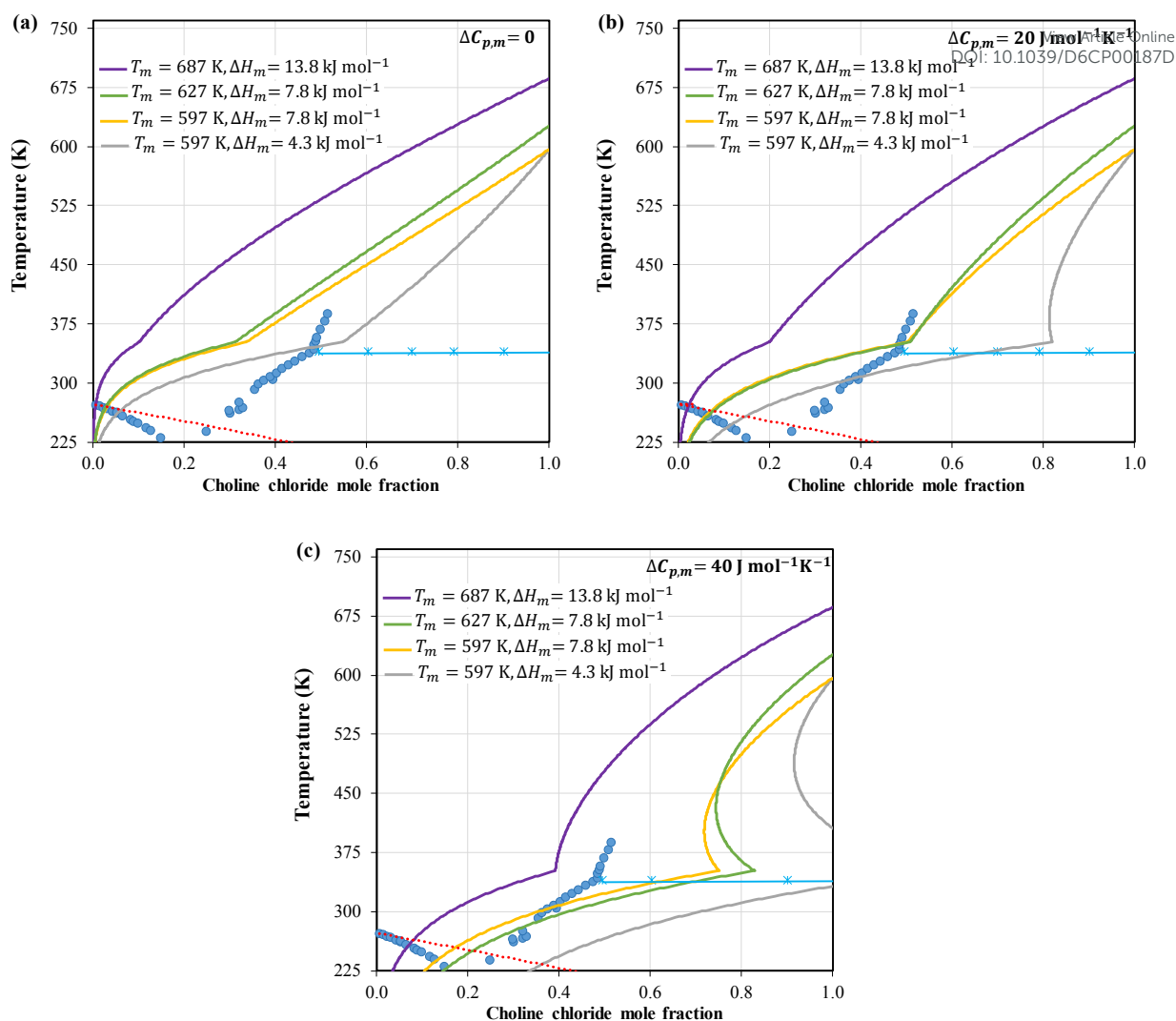


Figure 4. Solid-liquid phase diagram for the ChCl + water system: (a) $\Delta C_{p,m} = 0 \text{ J}\cdot\text{mol}^{-1}\cdot\text{K}^{-1}$, (b) $\Delta C_{p,m} = 20 \text{ J}\cdot\text{mol}^{-1}\cdot\text{K}^{-1}$, (c) $\Delta C_{p,m} = 40 \text{ J}\cdot\text{mol}^{-1}\cdot\text{K}^{-1}$, using the different melting properties compiled in Table 1: — Fernandez et al.⁷; — Vilas-Boas et al.³¹; — Bruinhorst et al.²⁴ and — Correa et al.³². ⋯ water solubility line, — solid-solid transition. ● and ✱ are data points from Lobo et al.²⁵

Figure 5 examines the influence of the melting enthalpy on the solubility lines of ChCl, using two different values of $\Delta C_{p,m}$ (Figure 5a, 5c and 5e, $\Delta C_{p,m} = 15 \text{ J mol}^{-1}\text{K}^{-1}$, and Figure 5b, 5d, and 5f, $\Delta C_{p,m} = 30 \text{ J mol}^{-1}\text{K}^{-1}$) across the reported melting temperature range. Within an amplitude of 90 K (range of the reported melting temperature from 597 to 687 K), the solubility lines exhibit minimal variation, provided all other melting properties remain constant. However, when higher melting temperatures are paired with the lowest melting enthalpy,⁷ the resulting solubility lines become defective. These lines display significant positive deviations from ideality and, as previously noted, show growing physical inconsistencies with increasing values of $\Delta C_{p,m}$. It is important to highlight that as the melting enthalpy increases, the system exhibits a more pronounced negative deviation from ideality. This leads to a shift in the eutectic point towards



lower ChCl mole fractions ($x_{E,ChCl}$) and significantly higher eutectic temperatures (T_E) compared to experimental observations ($x_{E,ChCl} = 0.20$ and $T_E = 204$ K).²⁵ Notably, the experimental solubility data above the solid-solid transition point are closer to the ChCl solubility line within the range of the melting enthalpies between 7.8 and 10.8 kJ mol⁻¹, as shown in Figure 5.

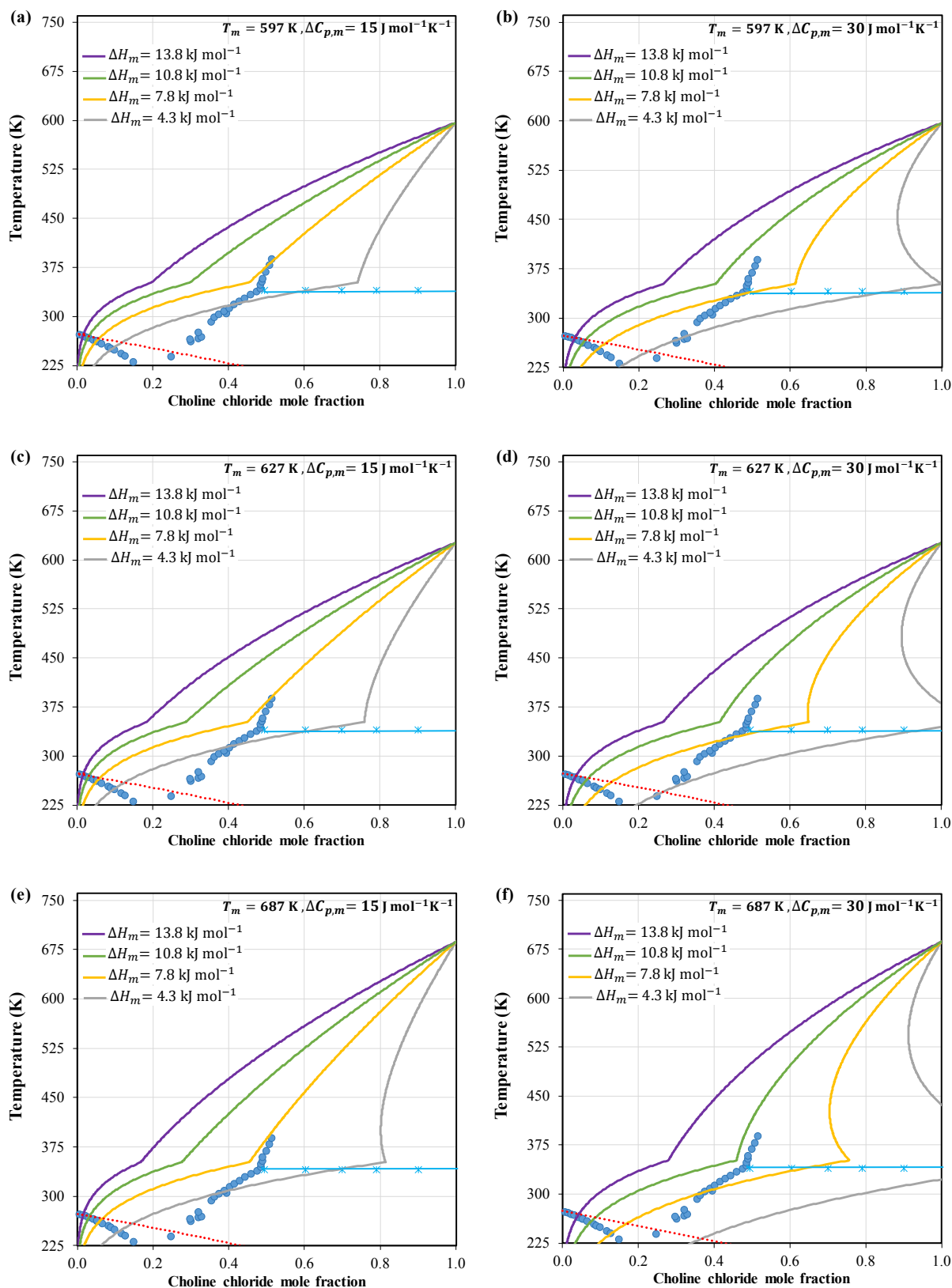


Figure 5. Solid-liquid phase diagram for the ChCl + water system for different melting enthalpies: $\Delta H_m = 4.3 \text{ kJ mol}^{-1}$; $\Delta H_m = 7.8 \text{ kJ mol}^{-1}$; $\Delta H_m = 10.8 \text{ kJ mol}^{-1}$ and $\Delta H_m = 13.8 \text{ kJ mol}^{-1}$. The solid lines represent the water solubility line, the dashed lines represent the solid-solid transition. The squares and circles are data points from Lobo et al.²⁵

ChCl + urea system

The same procedure was applied to the ChCl + urea system (Figure 6). It was observed that, depending on the values of the melting enthalpy and temperature, there is a threshold value of $\Delta C_{p,m}$ beyond which the phase diagram yields unrealistic representations. Since the melting temperature has a relatively minor influence on the overall phase diagram, representations are displayed at 597 K and 687 K using two different $\Delta C_{p,m}$ values. For a ChCl melting temperature of 597 K, the most suitable melting enthalpy to represent the SLE phase diagram lies between 7.8 and 10.8 kJ mol^{-1} .

In contrast to the ChCl + water system, where the highest experimentally reported mole fraction of ChCl was 0.515, for the ChCl + urea system, data points are available until a composition of $x_{\text{ChCl}} = 0.898$. At this composition, the solubility line is not expected to deviate significantly from the ideal solution solubility line. This is observed when using a melting temperature of 597 K and an enthalpy of fusion of 7.8 kJ mol^{-1} , consistent across both used values of $\Delta C_{p,m}$. Despite the high uncertainty in the experimental data, often attributed to residual water in the mixture or degradation due to temperature effects, the most appropriate range of the melting enthalpy to model the SLE phase diagram appears to be between 7.8 and 10.8 kJ mol^{-1} when the melting temperature is 687 K. However, such a high melting temperature would present substantial negative deviations from ideality, particularly at high ChCl mole fractions, which is not expected. These deviations become even more pronounced when an enthalpy of fusion of 13.8 kJ mol^{-1} is used.



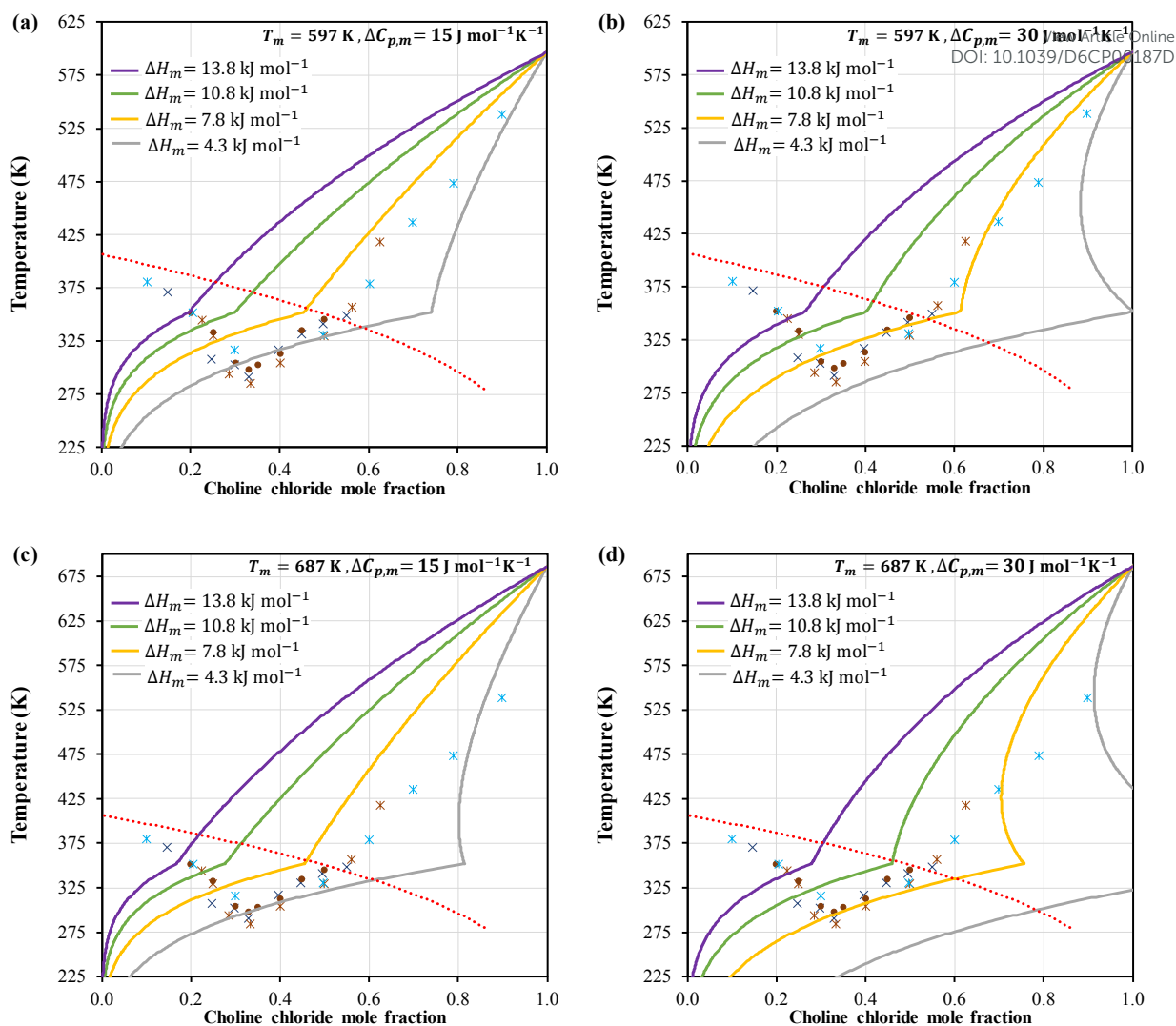


Figure 6. Solid-liquid phase diagram for the ChCl + urea system at different melting enthalpies: $\Delta H_m = 4.3 \text{ kJ mol}^{-1}$; $\Delta H_m = 7.8 \text{ kJ mol}^{-1}$; $\Delta H_m = 10.8 \text{ kJ mol}^{-1}$ and $\Delta H_m = 13.8 \text{ kJ mol}^{-1}$. \square urea solubility line. Experimental data were taken from: \times Abbot et al.¹ \ast Morrison et al.³³ \bullet Meng et al.³⁴ \times Silva et al.³⁵.

Non-Ideal Phase Diagrams

The previous analysis assumes the ideal solution behavior, which provides hints for the most probable range of melting properties of ChCl and helps to understand the impact of the melting enthalpy, heat capacity change, and melting temperature on the calculated phase diagram. Nevertheless, for an accurate representation of the ChCl + water and ChCl + urea SLE phase diagrams, the solution nonideality must be taken into account. For ChCl + urea, ChCl was assumed as a neutral ion pair. On the other hand, two approaches based on the NRTL model were implemented to estimate the activity coefficients of components in the liquid phase for ChCl + water: (1) modelling ChCl as a neutral ion pair or (2) modelling ChCl as fully dissociated ions, adding in this case a Pitzer-Debye Hückel long-range term. Recent work by Marques et al.³⁶



reported that considering the long-range ionic interactions improves the modelling of IL solutions.

View Article Online
DOI: 10.1039/D6CP00187D

For the ChCl + water system, different types of data sets are available in the literature, namely, vapor-liquid equilibrium (VLE),³⁷⁻³⁹ water activity,^{40, 41} heat of mixing,⁴² and mean ionic activity coefficient of ChCl from isopiestic measurements,⁴³⁻⁴⁵ which were used to estimate the NRTL binary parameters. Due to the observed interrelation between the melting properties and the solution nonideality, the experimental SLE data for the ChCl + water system were not used for parameter estimation. Details on the modelling approaches and the estimation of binary parameters are provided in the electronic supplementary information (ESI). The NRTL binary parameters for ChCl + water are presented in Table S1 of the ESI.

In contrast, only SLE data are available for the ChCl + urea mixture. Consequently, the melting enthalpy of ChCl and the NRTL binary parameters for the ChCl + urea system were determined by fitting to SLE data for both the ChCl + urea and ChCl + water systems. In this procedure, the NRTL binary parameters for ChCl + water were fixed to values previously estimated from non-SLE experimental data. The NRTL binary parameters for ChCl + urea and the estimated melting enthalpy values of ChCl can be found in Tables S2 and S3 in the ESI, respectively. The urea activity calculated at the eutectic composition (urea mole fraction of 0.67) at various temperatures is of the correct order of magnitude compared to experimental data (see Figure S2 in the ESI),⁴⁶ confirming the reliability of the estimated binary parameters for ChCl + urea. The root-mean-square deviation between experimental and calculated data can be found in Table S4 in the ESI.

Figure 7a shows the melting enthalpy of ChCl estimated in this work, assuming the different melting temperatures reported for ChCl (Table 1) and the heat capacity change upon melting for ChCl. As shown in Figure 7a, the ion pair (dashed line) and dissociated ions (solid lines) representation of ChCl yield very similar melting enthalpies. The melting enthalpy increases as $\Delta C_{p,m}$ increases. On the other hand, the melting temperature only slightly influences the values of ChCl melting enthalpy. In general, the estimated melting enthalpy at $\Delta C_{p,m} = 15 \text{ J mol}^{-1}\text{K}^{-1}$ (blue lines) is in good agreement with those reported by Vilas-Boas et al.³¹ (orange cross) and Correa et al.,³² (yellow cross) at $T_m = 597$ and 627 K , respectively. On the other hand, the estimated melting enthalpy at $\Delta C_{p,m} = 30 \text{ J mol}^{-1}\text{K}^{-1}$ (purple line) and $T_m = 687 \text{ K}$ is slightly lower than that found experimentally by van den Bruinhost et al.²⁴ (blue cross). Moreover, the estimated melting enthalpy at $\Delta C_{p,m} = 0$ (grey line) and $T_m = 597 \text{ K}$ is slightly higher than that reported by Fernandez et al.⁷ (green cross). As can be observed in Figure 7b, the calculated



melting entropy indicates that the estimated melting enthalpies fulfil Timmerman's criterion for the melting entropy of plastic crystalline materials (i.e., $\Delta S_m/R \leq 2$).⁴⁷

View Article Online
DOI: 10.1039/D6CP00187D

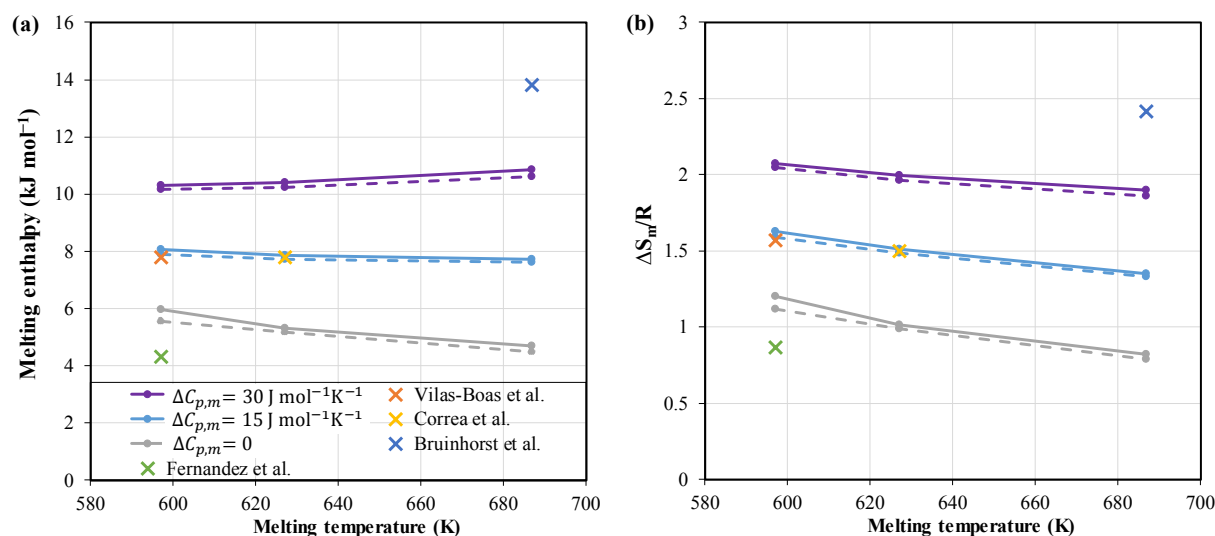


Figure 7. Choline chloride (ChCl) melting enthalpy (a) and entropy (b) estimated in this work, assuming different melting temperatures and heat capacity change of ChCl. Solid lines are data calculated when regarding ChCl as dissociated ions, and dashed lines are data calculated when considering ChCl as ion pairs in ChCl + water. Symbols represent melting properties of ChCl obtained from Fernandez et al.⁷ (green cross), Vilas-Boas et al.³¹ (orange cross), Correa et al.³² (yellow cross), and van den Bruinhorst et al.²⁴ (blue cross).

Although the estimated melting enthalpies are similar when assuming different modelling approaches or ChCl heat capacity change, the activity coefficients of ChCl in ChCl + water are different when regarding ChCl as ion pairs or dissociated ions (see Figure S1a in ESI, and Figures S1b for water activity, S1c to S1e for bubble-points, S1f for freezing point depression and S1g for partial molar excess enthalpy). Thus, the calculated liquidus line of ChCl using the ion pair or dissociated ions modelling approaches can be different, as the liquidus line is influenced by ChCl activity coefficients in the liquid phase.

Figure 8 shows the SLE phase diagram of ChCl + water system modelled assuming ChCl as ion pairs (Figure 8a, c, e) or fully dissociated ions (Figure 8b, d, f) and considering the different melting properties of ChCl. As shown in Figure 8, the influence of ChCl melting temperature on its calculated liquidus line is only noticeable at high mole fractions of ChCl. Nevertheless, at lower mole fractions of ChCl, increasing its melting temperature slightly shifts the liquidus and solidus lines to lower temperatures, in particular, as $\Delta C_{p,m}$ increases. When assuming ChCl as an ion pair (Figure 8a, c, and e), ChCl liquidus data are better represented as $\Delta C_{p,m}$ and T_m are lower (Figure 8a), while the eutectic point is more accurately predicted at a higher $\Delta C_{p,m}$ and T_m (Figure 8e). In contrast, assuming ChCl as dissociated ions (Figure 8b, d, and f) allows for representing the liquidus data at high $\Delta C_{p,m}$ and T_m (Figure 8f). Nevertheless, the eutectic



temperature is significantly underestimated when assuming ChCl as dissociated ions and considering high melting temperature and heat capacity change upon melting (Figure 8). This underestimation might result from extrapolating the Debye-Hückel parameter to extremely low temperatures. The Debye-Hückel parameter used in this work was adopted from Clarke and Glew,⁴⁸ which is calculated from experimental density and permittivity of water from 273.1 to 423.1 K, while the eutectic temperature of the system is close to 204 K. Neither of the modelling approaches can adequately represent liquidus data above the solid-solid transition temperature of ChCl .

View Article Online
DOI: 10.1039/C6CP01872D



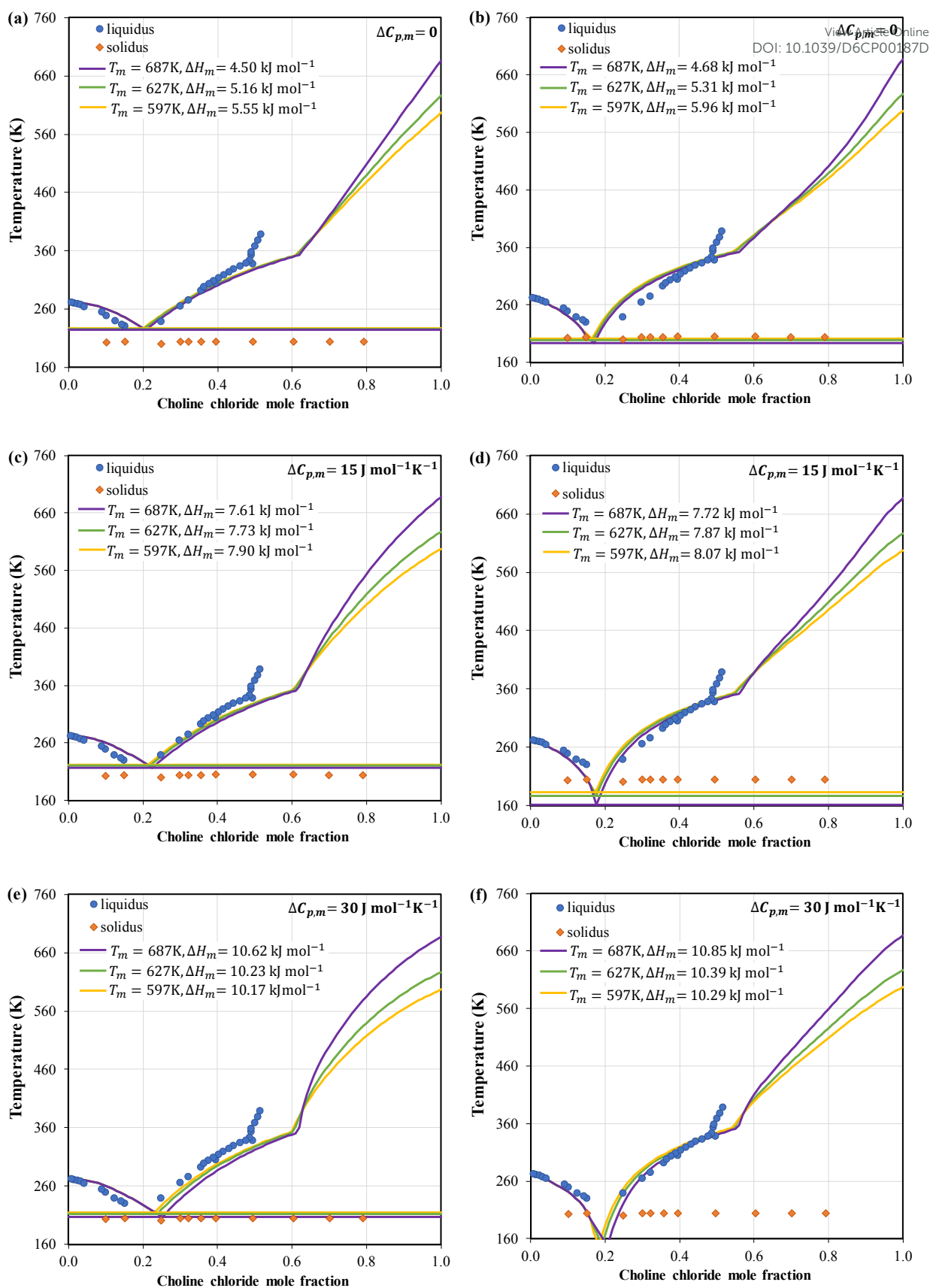


Figure 9 shows the activity coefficients of ChCl in the ChCl + water system calculated from the experimental liquidus temperature (symbols) and using the NRTL model (lines). Dashed lines represent activity coefficients of ChCl when it is regarded as ion pairs, while solid lines represent those when ChCl is considered as dissociated ions. The activity coefficients are calculated using the estimated melting enthalpy at each melting temperature together with the heat capacity change of ChCl. Because the estimated melting enthalpies when considering ChCl association or dissociation are similar (see Figure 7), those estimated considering ChCl dissociation were used to calculate the activity coefficients from the experimental data (ΔH_m in Figure 8b, d, and f).

As shown in Figure 9, treating ChCl as dissociated ions (solid lines) improves the description of ChCl activity coefficients at high ChCl mole fractions, whereas assuming ChCl to be as ion pairs (dashed lines) provides a better representation at low ChCl mole fractions. The calculated activity coefficients from the NRTL model assuming ChCl dissociation agree more closely with the activity coefficients derived from experimental data at $T_m = 687$ K and $\Delta C_{p,m} = 30$ J mol⁻¹K⁻¹ (blue crosses and solid lines in Figure 9c). The estimated melting enthalpy ($\Delta H_m = 10.85$ kJ mol⁻¹) at this $\Delta C_{p,m}$ and T_m is closer to that measured by van den Bruinhorst et al.²⁴ ($\Delta H_m = 13.8 \pm 3.0$ kJ mol⁻¹). On the other hand, a good description of ChCl activity coefficients could be observed when ChCl is regarded as ion pair and $T_m = 597$ K and $\Delta C_{p,m} = 15$ J mol⁻¹K⁻¹ (green circles and dashed lines in Figure 9e). The estimated melting enthalpy ($\Delta H_m = 7.90$ kJ mol⁻¹) at this melting temperature and heat capacity change is consistent with that estimated by Vilas-Boas et al.³¹ ($\Delta H_m = 7.80$ kJ mol⁻¹).

As expected from the observations in Figure 8, the activity coefficients calculated from experimental liquidus data above the solid-solid transition of ChCl cannot be described using any combination of $\Delta C_{p,m}$ and T_m in the studied range. In addition, the activity coefficients calculated from experimental data above the solid-solid transition using $T_m = 687$ K and $\Delta C_{p,m} = 30$ J mol⁻¹K⁻¹ seem implausible. This could be attributed to the shift in the solid-solid transition of ChCl in the presence of water. Lobo Ferreira et al.²⁵ showed that the ChCl solid-solid transition temperature shifts to around 340 K in ChCl + water, a value about 12 K lower than that of pure ChCl in the absence of water. Thus, the implausible activity coefficients calculated from the liquidus data below the solid-solid transition could in reality correspond to data above the solid-solid transition temperature.



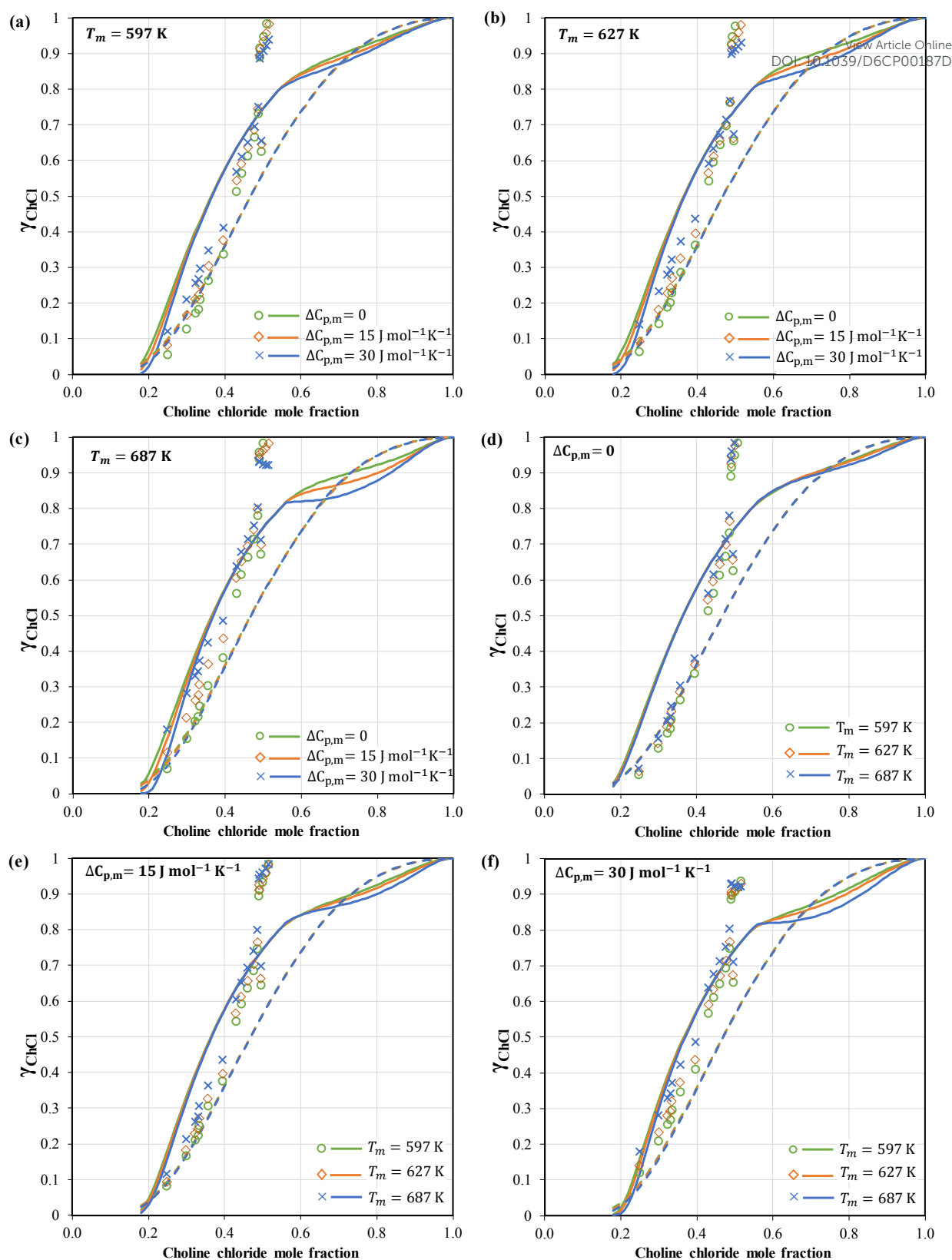


Figure 9. Activity coefficients of choline chloride (ChCl) in ChCl + water calculated at the liquidus temperature assuming ChCl as ion pairs (dashed lines) or fully dissociated ions (solid lines). The melting enthalpies estimated when modelling ChCl as dissociated ions were used to calculate the activity coefficients from experimental liquidus temperatures (symbols). Experimental data were taken from Lobo Ferreira et al.²⁵.



As the melting enthalpy was estimated using experimental ChCl solubility lines data from ChCl + water and ChCl + urea simultaneously, Figure 10 presents the SLE phase diagram of ChCl + urea calculated using the NRTL binary parameters for ChCl + urea (see Table S3). Although ChCl is always regarded as an ion pair in ChCl + urea, two different sets of binary NRTL parameters were obtained when ChCl in ChCl + water is assumed as ion pairs (Figure 10a, c, and e) or fully dissociated ions (Figure 10b, d, and f). The resulting binary parameters for ChCl + urea are nearly identical for both assumptions (see Table S2 in ESI), indicating that the main differences between the models when calculating the liquidus line of ChCl originate from the distinct $\Delta C_{p,m}$ and T_m used for ChCl. As previously observed for ChCl + water (Figure 8), the melting temperature has a stronger effect on the calculated ChCl liquidus line at high mole fractions of ChCl. In particular, only a melting temperature of $T_m = 597$ K (yellow lines in Figure 10) yields a satisfactory correlation of the liquidus curve near the melting point of pure ChCl. However, the influence of $\Delta C_{p,m}$ and T_m on the calculated liquidus line is less pronounced for the ChCl+urea than in the ChCl + water system (Figure 8). In general, a better agreement between the modelled and experimental ChCl liquidus and solidus lines in ChCl + urea is observed when $\Delta C_{p,m} = 0 \text{ J mol}^{-1}\text{K}^{-1}$.

View Article Online
DOI: 10.1039/C6PY0147D

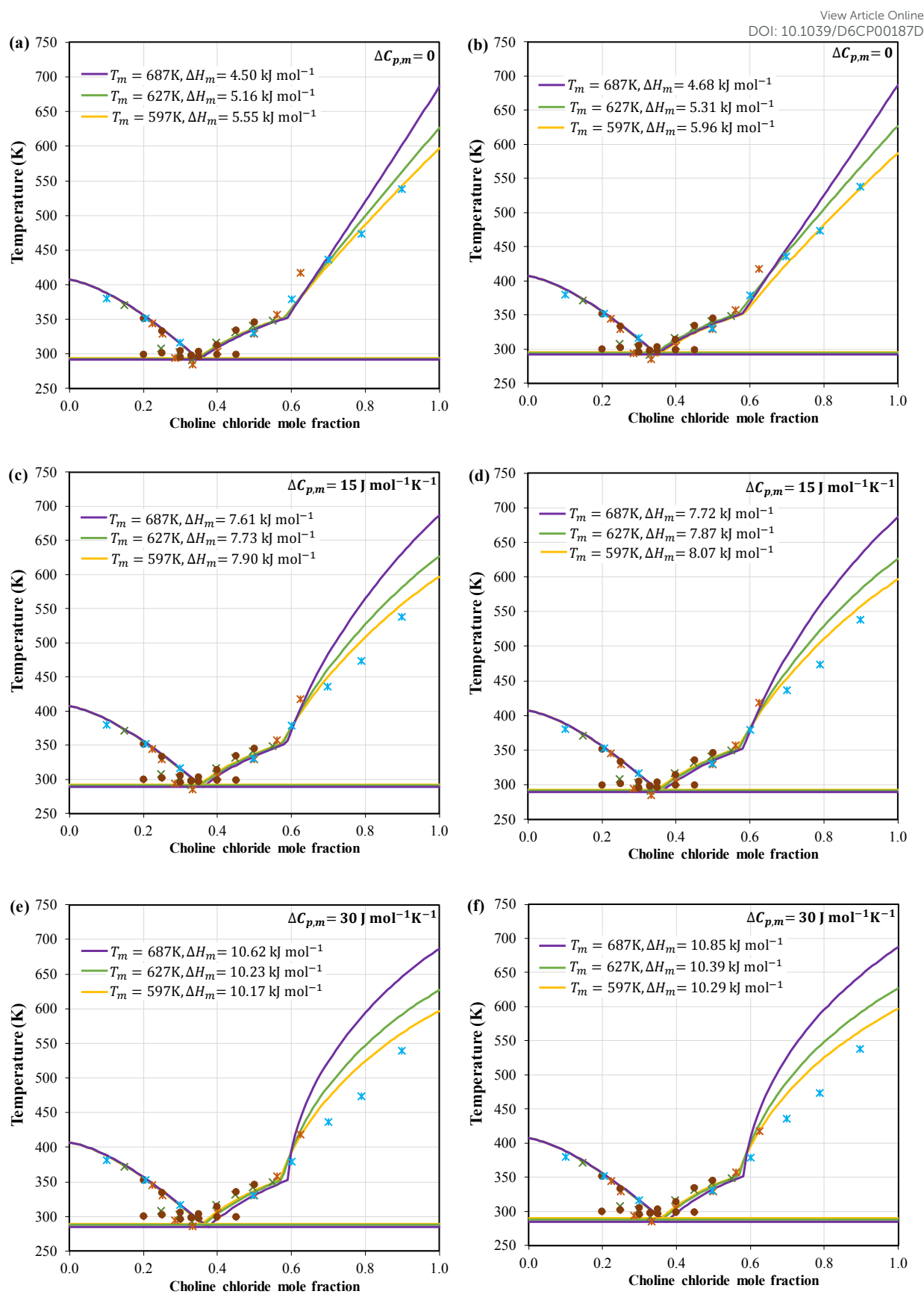






Figure 10. Solid-liquid equilibrium phase diagram of choline chloride ChCl + urea. ChCl is always regarded as a neutral ion pair in ChCl + urea, while for the ChCl + water is modeled as ion pairs (a), (c), and (e) or fully dissociated ions (b), (d), and (f). The melting enthalpy (ΔH_m) used for the modelling the ChCl liquidus line was



estimated in this work. Experimental data were taken from:  Abbot et al.¹  Morrison et al.³³  Meng et al.³⁴
 Silva et al.³⁵.

View Article Online
DOI: 10.1039/D6CP00187D

Figure 11 shows ChCl activity coefficients calculated at the experimental liquidus data (symbols) and predicted by the NRTL model (solid lines). As before, the activity coefficients were calculated using the NRTL binary parameters and the estimated melting enthalpy when ChCl is regarded as dissociated ions in ChCl + water (see Tables S2 and S3 in ESI). Unlike the behavior observed for ChCl + water, ChCl activity coefficients in the ChCl + urea system are best reproduced when the $T_m = 597$ K and $\Delta C_{p,m} = 0$ J mol⁻¹K⁻¹ (Figure 11a). Neither a large $\Delta C_{p,m}$ nor a high T_m allows for accurately predicting the ChCl activity coefficients in mixtures concentrated with ChCl (Figure 11c and f). Moreover, the influence of the T_m is more pronounced when $\Delta C_{p,m}$ is larger. As shown in Figure 11, the combination of $T_m = 597$ K and $\Delta C_{p,m} = 0$ J mol⁻¹K⁻¹ (Figure 11a) provides the most reliable description of ChCl activity in the ChCl + urea system. The corresponding melting enthalpy ($\Delta H_m = 5.95$ kJ mol⁻¹) is between the melting enthalpy estimated by Fernandez et al.⁷ ($\Delta H_m = 4.3$ kJ mol⁻¹) and Vilas-Boas et al.³¹ ($\Delta H_m = 7.80$ kJ mol⁻¹).



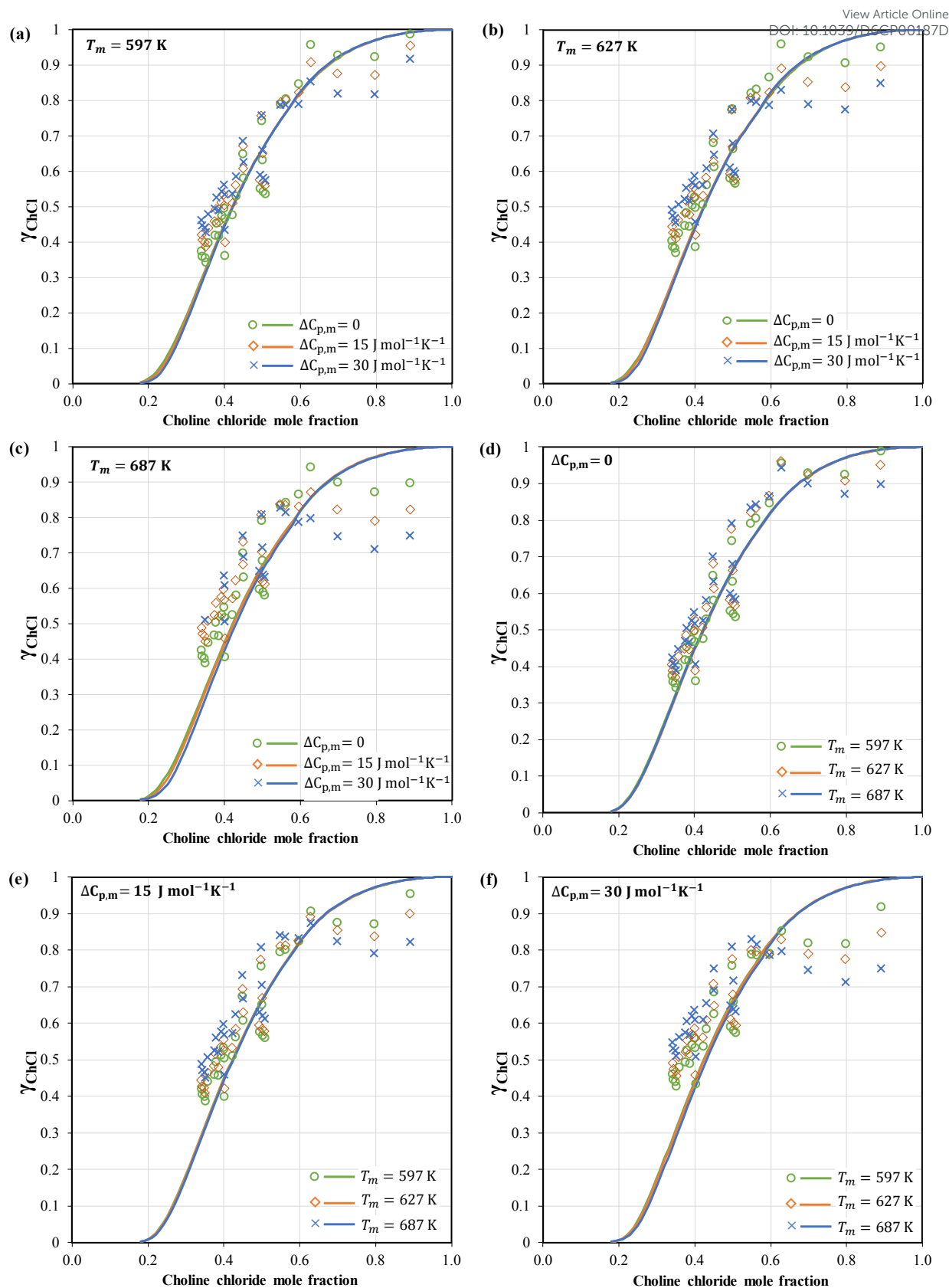


Figure 11. Activity coefficients of choline chloride (ChCl) in ChCl + urea calculated at the liquidus temperature using the estimated melting enthalpy at each melting temperature and heat capacity change. Experimental data were taken from: Abbot et al.,¹ Morrison et al.,³³ Meng et al.,³⁴ and Silva et al.³⁵



Because the ChCl heat capacity change upon melting largely influences the estimated melting enthalpy (Figure 7), it might be necessary to fit the $\Delta C_{p,m}$, along with its melting enthalpy and the NRTL binary parameters for ChCl + urea, to the SLE data of ChCl + urea and ChCl + water. Figure 12 shows the melting enthalpy and heat capacity change of ChCl fitted to the SLE data of ChCl + urea and ChCl + water when assuming ChCl as ion pairs or dissociated ions in ChCl + water (see Table S5 in ESI for the data). As shown in Figure 12, both the estimated melting enthalpy and heat capacity change decrease as the assumed melting temperature increases. When $T_m = 687$ K, considering $\Delta C_{p,m} = 0$ J mol⁻¹K⁻¹ is a more reasonable assumption. This behaviour is observed for ChCl + urea (Figure 10) and not in ChCl + water (Figure 8). The improved agreement obtained by neglecting $\Delta C_{p,m}$ can be attributed to the solubility data in ChCl + urea at higher ChCl mole fraction, where larger deviations from the experimental liquidus line occur in this region when $T_m = 687$ K (Figure 11). The choice of modelling approach (ion pairs or fully dissociated ions) has little impact on the estimated melting enthalpy, but it leads to significant differences in the estimated $\Delta C_{p,m}$. The estimated melting enthalpy at $T_m = 597$ K is consistent with that estimated by Vilas-Boas et al.³¹

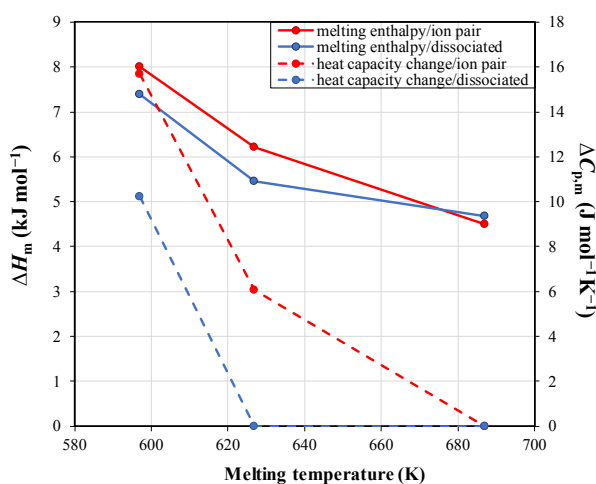


Figure 12. The melting enthalpy (ΔH_m) and heat capacity change ($\Delta C_{p,m}$) of choline chloride (ChCl) fitted to experimental solid-liquid equilibria data of ChCl + urea and ChCl + water regarding ChCl as ion pairs or fully dissociated ions.

Conclusions

This work critically evaluates the melting properties of ChCl and demonstrates their crucial influence on the thermodynamic description of SLE in ChCl-based *DES*. The wide dispersion of the ChCl melting temperatures and enthalpies reported in the literature is shown to directly affect



the modeling of SLE phase diagrams, calculated eutectic coordinates, and the interpretation of liquid-phase nonideality.

View Article Online
DOI: 10.1039/D6CP00187D

An essential outcome of this work is that neglecting the ChCl heat capacity change upon melting can lead to a systematic underestimation of its melting enthalpy. When the melting enthalpy is low, the heat capacity term makes a significant contribution to the calculated liquidus line of ChCl and cannot be ignored without compromising its physical consistency.

Comparative analysis of ideal and non-ideal SLE representations of ChCl + water and ChCl + urea reveals a strong interdependence between the melting properties of ChCl and its activity coefficients in the liquid phase. Low ChCl melting enthalpies artificially enforce ideal systems behaviour, while excessively high values require unrealistically strong negative deviations from ideality. Across ionic systems, including ChCl + water and ChCl + urea mixtures, melting enthalpy values between 8 and 10 kJ mol⁻¹, combined with a non-negligible heat capacity change upon melting in the range 20-40 J mol⁻¹K⁻¹ (decreasing with increasing melting temperature), provide the most consistent and physically meaningful description of the experimental SLE data.

Overall, this study emphasises that the reliable melting properties of ChCl are crucial for accurately interpreting ChCl-based *DES* phase diagrams and for developing robust thermodynamic and data-driven models. The conclusions drawn here provide practical guidance for selecting and validating melting properties in future research.



Author contribution

Ahmad Alhadid: Conceptualization, Investigation, Methodology, Formal Analysis, Data Curation, Writing – Original Draft. **Mirjana Minceva:** Conceptualization, Formal Analysis, Resources, Writing – Review & Editing. **João A. P. Coutinho:** Conceptualization, Formal Analysis, Writing – Review & Editing. **Simão P. Pinho:** Conceptualization, Investigation, Methodology, Formal Analysis, Data Curation, Writing – Original Draft, Supervision.

View Article Online

DOI: 10.1039/D6CP00187D

Declaration of Interests

The authors declare no conflict of interest.

Data Availability

Data supporting the work findings are available in the manuscript and the Supplementary Material file.

Statement on the use of AI tools

The authors declare that no artificial intelligence tools were used in the preparation of this manuscript.

Acknowledgements

This work was developed within the scope of the project CIMO-Centro de Investigação de Montanha, UIDB/00690/2020 (DOI: 10.54499/UIDB/00690/2020), UIDP/00690/2020 (DOI: 10.54499/UIDP/00690/2020); and SusTEC, LA/P/0007/2020 (DOI: 10.54499/LA/P/0007/2020), and CICECO-Aveiro Institute of Materials, UIDB/50011/2020 (DOI 10.54499/UIDB/50011/2020), UIDP/50011/2020 (DOI 10.54499/UIDP/50011/2020) & LA/P/0006/2020 (DOI 10.54499/LA/P/0006/2020), all financed by national funds through the FCT/MCTES (PIDDAC). The financial support from IUPAC Project No. 2022-002-2-500 is highly acknowledged.



References

1. A. P. Abbott, G. Capper, D. L. Davies, R. K. Rasheed and V. Tambyrajah, *Chem. Commun.*, 2003, 70-71.
2. B. B. Hansen, S. Spittle, B. Chen, D. Poe, Y. Zhang, J. M. Klein, A. Horton, L. Adhikari, T. Zelovich, B. W. Doherty, B. Gurkan, E. J. Maginn, A. Ragauskas, M. Dadmun, T. A. Zawodzinski, G. A. Baker, M. E. Tuckerman, R. F. Savinell and J. R. Sangoro, *Chem. Rev.*, 2021, **121**, 1232-1285.
3. E. L. Smith, A. P. Abbott and K. S. Ryder, *Chem. Rev.*, 2014, **114**, 11060-11082.
4. M. A. R. Martins, S. P. Pinho and J. A. P. Coutinho, *J. Solution Chem.*, 2019, **48**, 962-982.
5. M. S. Rahman, R. Roy, B. Jadhav, M. N. Hossain, M. A. Halim and D. E. Raynie, *J. Mol. Liq.*, 2021, **321**, 114745.
6. K.-S. Kim and B. H. Park, *J. Chem. Eng. Jpn.*, 2015, **48**, 881-884.
7. L. Fernandez, L. P. Silva, M. A. R. Martins, O. Ferreira, J. Ortega, S. P. Pinho and J. A. P. Coutinho, *Fluid Phase Equilib.*, 2017, **448**, 9-14.
8. B. P. Agbodekhe, M. N. Carlozo, D. O. Abranches, K. D. Jones, A. W. Dowling and E. J. Maginn, *Mol. Sys. Des. Eng.*, 2026, **11**, 85-106.
9. M. Farshad, F. Y. M. Salih, D. O. Abranches and Y. J. Colón, *J. Chem. Phys.*, 2025, **163**, 164118.
10. A. Bazyleva, W. E. Acree, V. Diky, G. T. Hefter, J. Jacquemin, M. C. F. Magalhães, J. W. Magee, D. K. Nordstrom, J. P. O'Connell, J. D. Olson, I. Polishuk, K. A. G. Schmidt, J. M. Shaw, J. P. M. Trusler and R. D. Weir, *Pure Appl. Chem.*, 2022, **94**, 1225-1247.
11. P. Pyykkö, *ChemPhysChem*, 2019, **20**, 123-127.
12. L. J. B. M. Kollau, M. Vis, A. van den Bruinhorst, A. C. C. Esteves and R. Tuinier, *Chem. Commun.*, 2018, **54**, 13351-13354.
13. A. Alhadid, L. Mokrushina and M. Minceva, *Molecules*, 2019, **24**, 2334.
14. Z. Song, J. Wang and K. Sundmacher, *Green Energy & Environ.*, 2021, **6**, 371-379.
15. D. Peng, A. Alhadid and M. Minceva, *Ind Eng Chem Res*, 2022, **61**, 13256-13264.
16. A. González de Castilla, J. P. Bittner, S. Müller, S. Jakobtorweihen and I. Smirnova, *J. Chem. Eng. Data.*, 2019, **65**, 943-967.
17. Z. Song, J. Chen, H. Qin, Z. Qi and K. Sundmacher, *Chem. Eng. Sci.*, 2023, **281**, 119097.
18. P. V. d. A. Pontes, E. Pereira, G. J. Maximo and E. A. C. Batista, *Fluid Phase Equilib.*, 2026, **601**, 114591.
19. K. Wang, M. Minceva and D. Peng, *Chem. Eng. Sci.*, 2026, **322**, 123130.
20. R. Wang, J. Chen, Z. Song and Z. Qi, *Ind Eng Chem Res*, 2023, **62**, 5382-5393.
21. L. B. Ayres, M. Bandara, C. D. McMillen, W. T. Pennington and C. D. Garcia, *ACS Sustain. Chem. Eng.*, 2024, **12**, 11260-11273.
22. A. K. Lavrinenko, I. Y. Chernyshov and E. A. Pidko, *ACS Sustain. Chem. Eng.*, 2023, **11**, 15492-15502.
23. F. J. López-Flores, C. Ramírez-Márquez, J. B. González-Campos and J. M. Ponce-Ortega, *Ind. Eng. Chem. Res.*, 2025, **64**, 3103-3117.



24. A. van den Bruinhorst, J. Avila, M. Rosenthal, A. Pellegrino, M. Burghammer and M. Costa Gomes, *Nat. Commun.*, 2023, **14**, 6684. View Article Online
DOI: 10.1039/D6CP00187D
25. A. I. M. C. Lobo Ferreira, S. M. Vilas-Boas, R. M. A. Silva, M. A. R. Martins, D. O. Abranches, P. C. R. Soares-Santos, F. A. Almeida Paz, O. Ferreira, S. P. Pinho, L. M. N. B. F. Santos and J. A. P. Coutinho, *Phys. Chem. Chem. Phys.*, 2022, **24**, 14886-14897.
26. P. Shanley and R. L. Collin, *Acta Crystallogr.*, 1961, **14**, 79-80.
27. J. M. Prausnitz, R. N. Lichtenthaler and E. G. d. Azevedo, *Molecular Thermodynamics of Fluid-Phase Equilibria*, Prentice Hall PTR, Upper Saddle River, NJ, 1999.
28. J. W. Kang, V. Diky, R. D. Chirico, J. W. Magee, C. D. Muzny, A. F. Kazakov, K. Kroenlein and M. Frenkel, *J. Chem. Eng. Data.*, 2014, **59**, 2283-2293.
29. L. P. Cunico, R. Ceriani, B. Sarup, J. P. O'Connell and R. Gani, *Fluid Phase Equilib.*, 2014, **362**, 318-327.
30. V. Petrouleas and R. M. Lemmon, *J. Chem. Phys.*, 1978, **69**, 1315-1316.
31. S. M. Vilas-Boas, D. O. Abranches, E. A. Crespo, O. Ferreira, J. A. P. Coutinho and S. P. Pinho, *J. Mol. Liq.*, 2020, **300**, 112281.
32. G. B. Correa, D. O. Abranches, E. Marin-Rimoldi, Y. Zhang, E. J. Maginn and F. W. Tavares, *J. Phys. Chem, Lett.*, 2024, **15**, 11801-11805.
33. H. G. Morrison, C. C. Sun and S. Neervannan, *Int. J. Pharm.*, 2009, **378**, 136-139.
34. X. Meng, K. Ballerat-Busserolles, P. Husson and J.-M. Andanson, *New J. Chem.*, 2016, **40**, 4492-4499.
35. L. P. Silva, C. F. Araújo, D. O. Abranches, M. Melle-Franco, M. A. R. Martins, M. M. Nolasco, P. J. A. Ribeiro-Claro, S. P. Pinho and J. A. P. Coutinho, *Phys. Chem. Chem. Phys.*, 2019, **21**, 18278-18289.
36. H. Marques, A. González de Castilla, S. Müller and I. Smirnova, *Fluid Phase Equilib.*, 2023, **569**, 113765.
37. M. Francisco, A. S. B. González, S. L. García de Dios, W. Weggemans and M. C. Kroon, *RSC Advances*, 2013, **3**, 23553-23561.
38. S. Gholami and A. Roosta, *J. Mol. Liq.*, 2019, **296**, 111876.
39. P. J. Carvalho, I. Khan, A. Morais, J. F. O. Granjo, N. M. C. Oliveira, L. M. N. B. F. Santos and J. A. P. Coutinho, *Fluid Phase Equilib.*, 2013, **354**, 156-165.
40. I. Khan, K. A. Kurnia, T. E. Sintra, J. A. Saraiva, S. P. Pinho and J. A. P. Coutinho, *Fluid Phase Equilib.*, 2014, **361**, 16-22.
41. P. Velho, E. Sousa and E. A. Macedo, *Fluid Phase Equilib.*, 2025, **587**, 114197.
42. A. van den Bruinhorst, C. Corsini, G. Depraetère, N. Cam, A. Pádua and M. Costa Gomes, *Faraday Discuss.*, 2024, **253**, 273-288.
43. R. Fleming, *J. Chem. Soc. (Resumed)*, 1961, 3100-3102.
44. J. B. Macaskill, M. S. Mohan and R. G. Bates, *Anal. Chem.*, 1977, **49**, 209-212.
45. G. E. Boyd, A. Schwarz and S. Lindenbaum, *J. Phys. Chem.*, 1966, **70**, 821-825.
46. F. I. Travaglini, L. Romagnoli, A. M. Czerska, M. Busato, G. Mannucci, S. Vecchio Cipriotti, P. D'Angelo and A. Cicciooli, *Phys. Chem. Chem. Phys.*, 2025, **27**, 25266-25270.
47. J. Timmermans, *J. Phys. Chem. Solids*, 1961, **18**, 1-8.



48. E. C. W. Clarke and D. N. Glew, *J. Chem. Soc., Faraday Trans. 1*, 1980, **76**, 1911-1916.

View Article Online
DOI: 10.1039/D6CP00187D



Data supporting the work findings are available in the manuscript and the Supplementary Material file.

[View Article Online](#)

DOI: 10.1039/D6CP00187D

